Article

Cell Reports

The Histone Demethylase KDM5 Activates Gene Expression by Recognizing Chromatin Context through Its PHD Reader Motif

Graphical Abstract

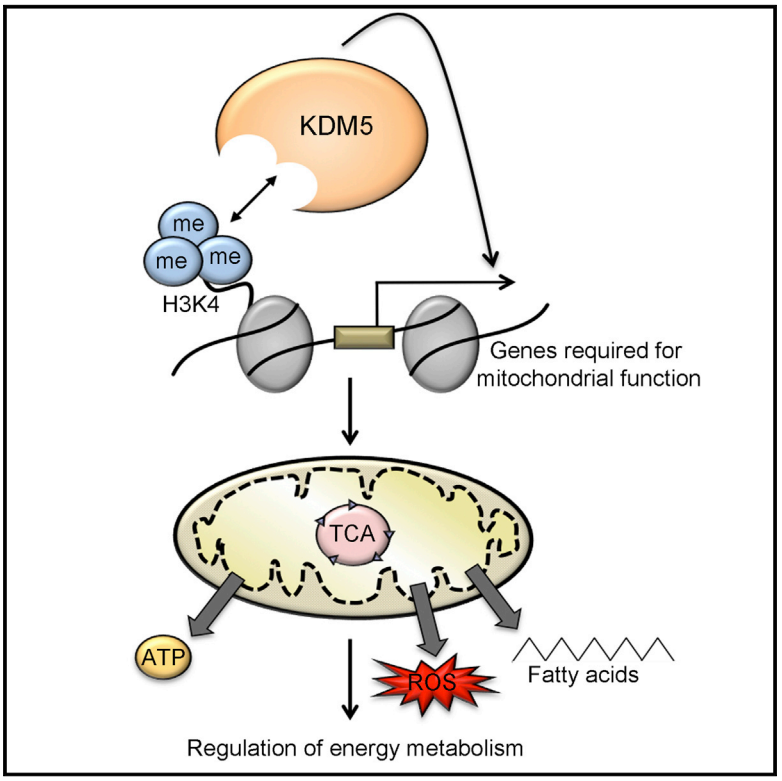

Authors

Xingyin Liu, Julie Secombe

Correspondence

julie.secombe@einstein.yu.edu

In Brief

KDM5 family proteins are critically important transcriptional regulators whose dysfunction is linked to cancer and intellectual disability. Liu and Secombe find that KDM5 activates genes critical for mitochondrial function and metabolism through recognition via its PHD domain.

Highlights

- KDM5 binding correlates with promoter regions enriched for H3K4me3
- KDM5 activates genes required for mitochondrial function
- *kdm5* mutants show metabolic defects related to mitochondrial dysfunction
- The H3K4me3-binding PHD motif of KDM5 plays a key role in gene activation

Accession Numbers

GSE70591

Liu & Secombe, 2015, Cell Reports *13*, 2219–2231
December 15, 2015 ©2015 The Authors
http://dx.doi.org/10.1016/j.celrep.2015.11.007

Cell Reports
Article

The Histone Demethylase KDM5 Activates Gene Expression by Recognizing Chromatin Context through Its PHD Reader Motif

Xingyin Liu[1] and Julie Secombe[1,*]
[1]Department of Genetics, Albert Einstein College of Medicine, 1300 Morris Park Avenue, Bronx, NY 10461, USA
*Correspondence: julie.secombe@einstein.yu.edu
http://dx.doi.org/10.1016/j.celrep.2015.11.007

SUMMARY

KDM5 family proteins are critically important transcriptional regulators whose physiological functions in the context of a whole animal remain largely unknown. Using genome-wide gene expression and binding analyses in *Drosophila* adults, we demonstrate that KDM5 (Lid) is a direct regulator of genes required for mitochondrial structure and function. Significantly, this occurs independently of KDM5's well-described JmjC domain-encoded histone demethylase activity. Instead, it requires the PHD motif of KDM5 that binds to histone H3 that is di- or trimethylated on lysine 4 (H3K4me2/3). Genome-wide, KDM5 binding overlaps with the active chromatin mark H3K4me3, and a fly strain specifically lacking H3K4me2/3 binding shows defective KDM5 promoter recruitment and gene activation. KDM5 therefore plays a central role in regulating mitochondrial function by utilizing its ability to recognize specific chromatin contexts. Importantly, KDM5-mediated regulation of mitochondrial activity is likely to be key in human diseases caused by dysfunction of this family of proteins.

INTRODUCTION

Regulation of gene expression is essential for cell fate specification, developmental processes, and maintenance of cellular homeostasis. KDM5 family proteins are important transcriptional regulators that activate or repress gene expression in a context-dependent manner. Mammalian cells encode four KDM5 paralogs, KDM5A (Rbp2, JARID1A), KDM5B (Plu1, JARID1B), KDM5C (SMCX, JARID1C), and KDM5D (SMCY, JARID1D), while *Drosophila* has a single KDM5 ortholog (Lid). Evidence that KDM5 family proteins play key gene regulatory roles comes from the observations that knockout of mouse KDM5B or *Drosophila* KDM5 results in lethality (Albert et al., 2013; Catchpole et al., 2011; Gildea et al., 2000). Moreover, dysregulation of KDM5 proteins in humans results in disease, with overexpression of KDM5 proteins being implicated in oncogenesis and their loss in cognitive impairment (Blair et al., 2011; Vallianatos and Iwase, 2015).

The most studied activity of KDM5 proteins is their Jumonji (JmjC) domain-encoded histone demethylase activity (Benevolenskaya, 2007). In mammalian cells and *Drosophila*, KDM5 proteins demethylate trimethylated histone H3 (H3K4me3), a chromatin mark characteristic of promoter regions of actively transcribed genes (Santos-Rosa et al., 2002). To date, most loss- and gain-of-function KDM5 phenotypes described have been attributed exclusively to their demethylase activity. However, studies of mouse KDM5B and *Drosophila* KDM5 demonstrate that demethylase-inactive animals develop normally to produce viable adults that are morphologically normal (Catchpole et al., 2011; Li et al., 2010). Consistent with this, we and others have shown demethylase-independent gene regulatory functions of KDM5 proteins (Benevolenskaya, 2007; Cao et al., 2014; DiTacchio et al., 2011; Lee et al., 2009). While this leaves the in vivo significance of KDM5's enzymatic activity uncertain, it emphasizes the functional importance of KDM5's other gene regulatory activities. For example, KDM5 family proteins affect transcription through interactions with lysine deacetylases (HDACs), leading to changes in the acetylation of histones and other proteins (Barrett et al., 2007; DiTacchio et al., 2011; Lee et al., 2009; Liu et al., 2014; Nishibuchi et al., 2014). Importantly, because KDM5 proteins have additional motifs with defined in vitro functions, additional gene regulatory mechanisms are likely to be crucial for KDM5 function in vivo. These include N- and C-terminal PHD motifs that bind to H3K4me0 and H3K4me2/3, respectively (Klein et al., 2014; Li et al., 2010; Torres et al., 2015; Wang et al., 2009). The binding activities of these two PHD motifs are particularly intriguing as they are the substrate and product of KDM5's demethylase activity, and it remains unclear whether they act independently or in a coordinated manner to affect transcription.

Dysfunction of transcriptional regulators is well established to lead to a large number of diseases. Indeed, loss-of-function mutations in KDM5A, KDM5B, or KDM5C are found in patients with intellectual disability, linking KDM5 function to cognition through unknown mechanism(s) (Vallianatos and Iwase, 2015). In addition, overexpression of KDM5A or KDM5B is implicated in the genesis and progression of several cancers, most notably melanoma, breast, gastric, lung, and prostate cancers (reviewed by Blair et al., 2011). While the precise roles of KDM5A and KDM5B in tumor development remain to be elucidated, their

A

Biological Process

Term	Gene count	*p*-value
Glycosylation	895	5.20E-19
Cellular lipid metabolic process	585	2.00E-17
Larval development	857	2.30E-17
Organic acid biosynthetic process	801	2.40E-16
Protein amino acid glycosylation	867	7.90E-16
Regulation of cell shape	727	1.40E-15
Regulation of cell morphogenesis	725	2.00E-13
Heart development	709	1.10E-13
Ectoderm development	736	1.90E-13
Lipid biosynthetic process	736	1.90E-13
Mitotic spindle elongation	557	6.90E-09
Spindle elongation	561	2.90E-08
Mitotic spindle organization	537	6.80E-08
Negative regulation of cell differentiation	490	7.50E-06

Cellular Component

Term	Gene count	*p*-value
Intracellular organelle	2736	5.80E-11
Intracellular membrane-bound organelle	2374	7.70E-09
Nucleus	1455	2.30E-06
Lipid particle	222	3.30E-05
Ribosomal subunit	150	3.60E-05
Organellar ribosome	72	3.80E-05
Mitochondrial ribosome	72	3.80E-05
Large ribosomal subunit	95	2.80E-04
Ribosome	165	7.60E-04
Plasma membrane part	346	7.60E-04
Nucleoplasm	229	2.00E-03
Mitochondrial matrix	139	2.70E-03
Mitochondrial lumen	139	2.70E-03
Cytoskeleton	299	2.80E-03

B

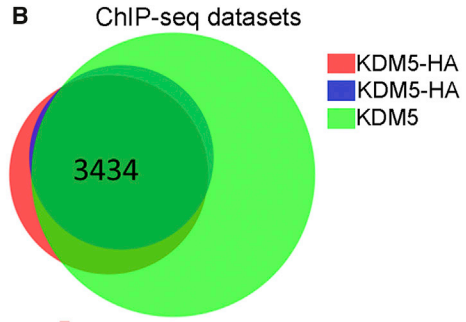

C

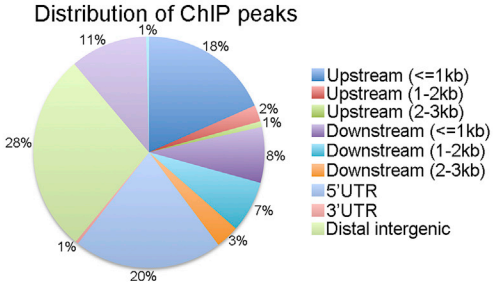

D

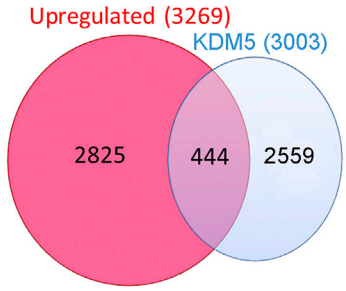

E

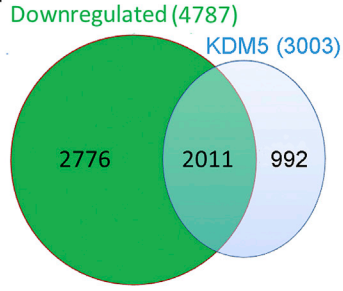

F

Biological Process

Term	Gene count	*p*-value
Cellular metabolic process	842	3.2E-54
Macromolecule metabolic process	711	1.2E-22
Organelle organization	284	4.5E-21
Primary metabolic process	818	8.1E-18
Nitrogen compound metabolic process	394	3.9E-16
Macromolecular complex subunit organization	105	9.8E-15
Cellular localization	163	1.4E-13
Vesicle-mediated transport	130	1.5E-13
Macromolecule localization	158	3.8E-13
Establishment of localization in cell	140	5.7E-13
Establishment of protein localization	100	3.9E-12
Regulation of cellular component organization	95	7.8E-11
Biosynthetic process	374	4.8E-10
Regulation of metabolic process	292	1.4E-09

Cellular Component

Term	Gene count	*p*-value
Intracellular organelle lumen	215	2.4E-18
Nuclear lumen	151	4.8E-13
Nucleoplasm part	147	1.8E-12
Ribonucleoprotein complex	101	4.4E-11
Lipid particle	98	6.6E-09
Cytoplasm	662	7.30E-08
Chromosome	103	1.20E-05
Ribosome	69	0.000017
Mitochondrial lumen	59	0.00005
Cytosolic ribosome	39	0.000067
Large ribosomal subunit	42	0.000067
Mitochondrial part	128	0.000091
Chromosomal part	81	0.00022
Cytoplasmic part	497	0.00054

G

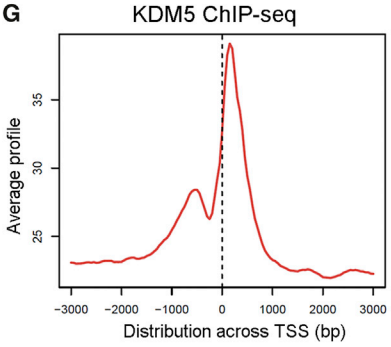

H

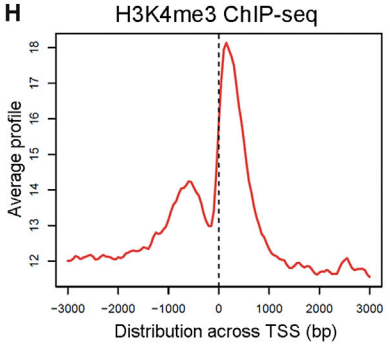

J

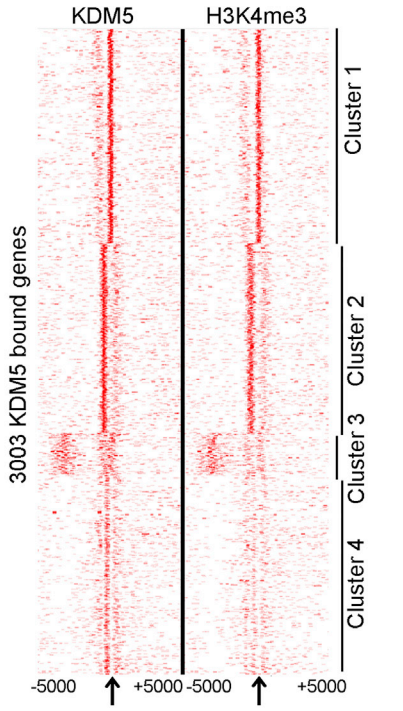

I

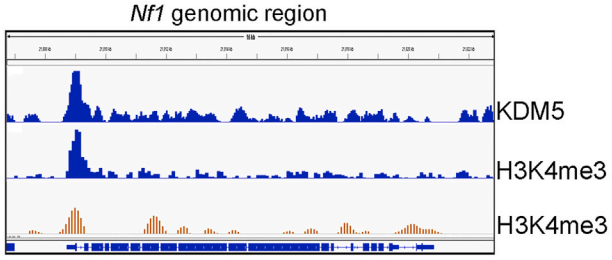

K

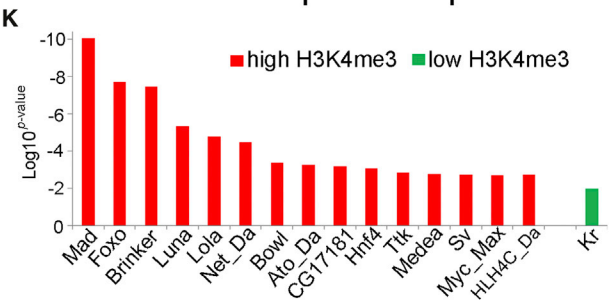

(legend on next page)

interactions with key tumorigenic factors such as the oncoprotein transcription factor Myc and the tumor suppressor pRB are likely to be important (Benevolenskaya, 2007; Outchkourov et al., 2013; Secombe et al., 2007). Interestingly, recent data support the idea that KDM5 proteins promote the growth and survival of a more slowly proliferating subset of cancer cells (Roesch et al., 2010, 2013; Sharma et al., 2010). Because standard therapies target rapidly dividing cells, this results in KDM5A- and KDM5B-overexpressing tumors being difficult to treat. Slow-growing KDM5-overexpressing tumor cells are also metabolically distinct from other tumor cells because they generate ATP through oxidative phosphorylation in the mitochondria and not via aerobic glycolysis (Roesch et al., 2013; Song et al., 2015). KDM5 proteins may, therefore, regulate fundamental metabolic processes related to energy production through unknown molecular mechanisms.

Key to understanding the biology of KDM5 proteins is defining their target genes and the mechanisms by which they regulate transcription. By combining genome-wide transcriptome and binding assays, we establish the repertoire of direct KDM5 target genes in *Drosophila* adults. Our analyses define KDM5 as a critical regulator of genes integral to mitochondrial structure and function. Significantly, the activation of critical mitochondrial genes does not require the JmjC domain-encoded demethylase activity of KDM5. Instead, it relies on its C-terminal PHD motif that binds to di- and trimethylated H3K4. Recognition of a specific chromatin context is, therefore, a critical means by which KDM5 activates the transcription of genes essential to mitochondrial function in vivo. Because altered mitochondrial activity is a feature of cancer cells and also is implicated in cognitive dysfunction, our data provide key insights into the means by which loss or gain of KDM5 family genes leads to human disease.

RESULTS

KDM5 Regulates Distinct Genes in Larvae and Adults

We previously demonstrated that larvae and adults with a hypomorphic combination of *kdm5* alleles ($kdm5^{K6801/10424}$) have 70% less KDM5 protein than wild-type and die more quickly than controls when exposed to the oxidizer paraquat (Liu et al., 2014). In *kdm5* mutant larvae, paraquat sensitivity correlates with the downregulation of at least 15 target genes that are co-regulated by KDM5 and the stress response transcription factor Foxo (Liu et al., 2014). In contrast to our findings in larvae, analyses of those same 15 target genes in *kdm5* mutant adults revealed that only six were downregulated, while six others were unaffected and three were upregulated (Figure S1A). KDM5 therefore regulates distinct targets during larval development and adulthood.

To identify KDM5-regulated genes in adults, we carried out RNA sequencing (RNA-seq) analyses of $kdm5^{K6801/10424}$ mutant flies and compared this to age-matched wild-type animals. (Figures S1B and S1C; Table S1). In unstressed conditions, *kdm5* mutant flies had 8,056 differentially expressed genes (DEGs). Of these, 4,787 genes were significantly downregulated and thus required KDM5 for their activation, while 3,269 genes were upregulated and so were normally repressed by KDM5 ($p < 0.05$, false discovery rate [FDR] < 0.05; Figures S1D and S1E). Similar to our previous microarray data from larval wing imaginal discs, many genes affected in *kdm5* hypomorphic mutant adults were altered 2-fold or less (Figure S2A; Liu et al., 2014). Analyses of KDM5-regulated genes (both up- and downregulated) revealed enrichment for a number of diverse biological processes (gene ontology [GO] categories), including glycosylation, lipid metabolism, and cell division (Figure 1A). DEGs were also implicated in the functioning of several subcellular compartments, including the mitochondria, ribosomes, and lipid particles (Figure 1A).

Because *kdm5* mutants are sensitive to the oxidizer paraquat, we tested whether KDM5 was required for the transcriptional response to this stressor. To do this, we carried out RNA-seq analyses of wild-type and *kdm5* mutant adults in oxidative stress conditions. Paraquat treatment of wild-type flies led to the upregulation of 2,481 genes and the downregulation of 3,103 genes ($\geq$1.5-fold, $p \leq 0.05$; Figures S2B and S2C). These included genes known to be activated by paraquat that are required to detoxify excess reactive oxygen species, such as glutathione S-transferase and cytochrome P450 genes (Zou et al., 2000). Paraquat-mediated changes to gene expression did not generally require KDM5 (Figures S2D–S2F). The *kdm5* mutant adult sensitivity to oxidative stress conditions is, therefore, due to defects that exist prior to stress conditions. We thus focused on gene expression changes and phenotypes observed in *kdm5* mutants in non-stressed conditions.

Figure 1. Genes Directly Regulated by KDM5 in Adults

(A) Analyses of RNA-seq data to identify enriched biological process and cellular component categories for genes with altered expression in *kdm5* mutant flies (up- and downregulated genes) are shown.

(B) Overlap between anti-HA (two replicates) and KDM5 ChIP-seq datasets ($q < 0.05$) is shown.

(C) Genomic distribution of KDM5 ChIP-seq peaks using anti-HA is shown.

(D) Comparison of RNA-seq and ChIP-seq data shows directly repressed genes.

(E) Directly activated genes are shown.

(F) GO analysis of directly regulated genes is shown.

(G) KDM5 ChIP-seq read density relative to the transcriptional start site (TSS) at DEGs is shown.

(H) H3K4me3 ChIP-seq read density relative to the TSS of KDM5-bound and regulated genes is shown.

(I) IGV genome browser view of *Nf1* showing overlapping KDM5 and H3K4me3 peaks. Middle (blue) H3K4me3 trace is data from our analyses; bottom (orange) H3K4me3 is published data (GEO: GSM400670).

(J) Heatmap shows distribution of KDM5 and H3K4me3 relative to TSS (clustered using k-means).

(K) Transcription factor binding sites enriched within KDM5 peaks using MEME-ChIP are shown. Mad, Mothers against decapentaplegic; Lola, Longitudinals lacking; Da, Daughterless; Bowl, brother of odd with entrails limited; Ato, Atonal; Hnf4, Hepatocyte nuclear factor 4; Ttk, Tramtrack; Kr, Krüppel.

KDM5 Binding Correlates with the Active Chromatin Mark H3K4me3

To determine which genes affected in *kdm5* hypomorphic mutant adults were direct targets, we carried out chromatin immunoprecipitation sequencing (ChIP-seq) analyses of wild-type adults using an anti-KDM5 antibody. To independently confirm these data, we utilized a fly strain in which the sole source of KDM5 is from a transgene expressing an HA-tagged form of KDM5 expressed under the control of its endogenous promoter (Liu et al., 2014). Analyses of two anti-HA datasets and one KDM5 ChIP-seq dataset revealed a total of 3,434 binding sites that were enriched at promoter regions (FDR < 0.05; Figures 1B and 1C; Figures S3A–S3C). These 3,434 KDM5-binding peaks mapped to 3,003 genes that were used for subsequent integration with RNA-seq analyses from *kdm5* mutant adults.

Of KDM5-bound genes, 15% were upregulated in *kdm5* mutant adults (444/3,003; Figure 1D). A much higher proportion of KDM5-bound genes were downregulated (2,011/3,003, 67%); thus, the primary function of KDM5 in adults is to activate gene expression (Figure 1E). GO analysis of these 2,455 directly regulated KDM5 target genes revealed enrichment for diverse metabolic processes and cellular compartments, including those required for mitochondrial function (Figure 1F). The remaining 548 KDM5-binding sites (18%) occurred at genes whose expression was unaltered in *kdm5* mutants. The function of KDM5 at these sites remains to be determined. Notably, consistent with our observation that paraquat-mediated changes to gene expression did not require KDM5, KDM5 binding was not altered by this stress condition (Figure S3D). These data confirm that the primary role of KDM5 is to regulate gene expression in normal, unstressed conditions.

The JmjC domain of KDM5 demethylates H3K4me3 and the C-terminal PHD motif (PHD3) binds to H3K4me2/3 (Li et al., 2010; Wang et al., 2009). We therefore investigated the link between KDM5 and H3K4me3 by carrying out anti-H3K4me3 ChIP-seq from wild-type adults and using a published modENCODE dataset (Nègre et al., 2011). KDM5 and H3K4me3 showed a similar distribution, peaking near transcription start sites (TSSs) (Figures 1G–1I; Figure S3E). Additional genome-wide analyses of ChIP-seq peak data revealed four clusters with distinct patterns and degrees of enrichment for KDM5 binding and H3K4me3 (Figure 1J; Figure S3F). Genes within clusters 1 and 2 showed higher levels of H3K4me3 and KDM5 binding primarily surrounding the TSSs and were more highly expressed. Genes in clusters 3 and 4 had lower levels of H3K4me3 and KDM5 binding and were expressed at low levels. At these genes, KDM5 and H3K4me3 were more dispersed and not limited to the TSS region. We also compared our KDM5 ChIP-seq data with three other published datasets that were generated using adult females: H3K9 acetylation (H3K9ac) that marks active promoters in addition to H3K4me1 and H3K27ac that are associated with enhancer elements. As expected based on the overlap between KDM5 and H3K4me3, KDM5 binding correlated with H3K9ac (Figure S4A). In contrast, KDM5 binding was not significantly correlated with H3K27ac or H3K4me1 (Figures S4B–S4F). KDM5 therefore primarily localizes to promoters.

Besides identifying additional KDM5 target genes, our data support the biological importance of previously published KDM5 interactions with transcription regulatory complexes. For example, MEME-ChIP web service (Machanick and Bailey, 2011) analyses of KDM5 ChIP peaks with high levels of H3K4me3 showed enrichment for Foxo- and Myc-binding sites that we and others have previously linked to KDM5 (Figure 1K; Liu et al., 2014; Outchkourov et al., 2013; Secombe et al., 2007). Binding sites for a number of other transcription factors also were enriched within KDM5-bound regions, including those that mediate TGF-β/BMP signaling (e.g., Mad, Brinker, and Medea) and neuronal development (e.g., Lola, Daughterless, and Tramtrack). In contrast to KDM5 peaks that had high H3K4me3, KDM5 peaks with lower levels of this chromatin mark showed enrichment for only one transcription factor binding site, the developmental regulator Kruppel (Figure 1K). KDM5 is therefore likely to be important for the regulation of several developmentally important pathways.

KDM5 Directly Regulates Genes Required for Mitochondrial Function

Our ChIP-seq and RNA-seq analyses revealed that KDM5 regulates genes involved in mitochondrial structure and function (Figure 2A). For example, among the direct targets that were downregulated in *kdm5* mutants were genes required for mitochondrial morphology (*deep orange* [*dor*], *twins* [*tws*], *Neurofibromin 1* [*Nf1*], and *bicoid-interacting protein 3* [*bin3*]), components of the inner or outer mitochondrial membrane (*no mitochondrial derivative* [*nmd*], *Pmi*, and *black pearl* [*blp*]), the mitochondrial chaperone *tumorous imaginal discs* (*l(2)tid*), and genes essential to mitochondrial tRNA function (the *Seryl tRNA synthase Slimp* and the Leucyl-tRNA synthase *Aats-leu*). Other genes integral to mitochondrial function were bound by KDM5 but did not show changes to transcript levels in *kdm5* mutants (e.g., *mitochondrial assembly factor* [*Marf*] and *fission1* [*Fis1*]) (Figure 2A). These may be regulated in a more tissue-restricted manner, so changes to their expression were not detectable using whole animals.

Because of their established roles in mitochondrial function, we focused on KDM5-dependent activation of *dor*, *Pmi*, *Slimp*, *tws*, *nmd*, *Nf1*, *l(2)tid*, *Aats-leu*, *blp*, and *bin3*, all of which showed KDM5 binding and the presence of H3K4me3 near the TSS (Figure 2B). To verify these ChIP-seq data, we confirmed KDM5 and H3K4me3 enrichment by ChIP-PCR (Figures 2C and 2D). We also examined H3K4me3 levels in *kdm5* mutant flies and found that, despite the decreased expression of these KDM5 target genes, promoter H3K4me3 levels were increased (Figure 2D). This is consistent with the histone demethylase activity of KDM5 and the observation by us and others that global levels of H3K4me3 are increased in *kdm5* mutants (Eissenberg et al., 2007; Lee et al., 2007; Secombe and Eisenman, 2007). It is also consistent with the notion that, while there is a correlation between H3K4me3 and increased transcription, there is not a causal relationship (Sims and Reinberg, 2006).

kdm5 Mutants Show Mitochondrial Defects, Altered Metabolism, and Increased Oxidative Stress

Because KDM5 directly regulates genes integral to mitochondrial structure and function, we examined *kdm5* mutants for phenotypes in the highly metabolically active thoracic muscles.

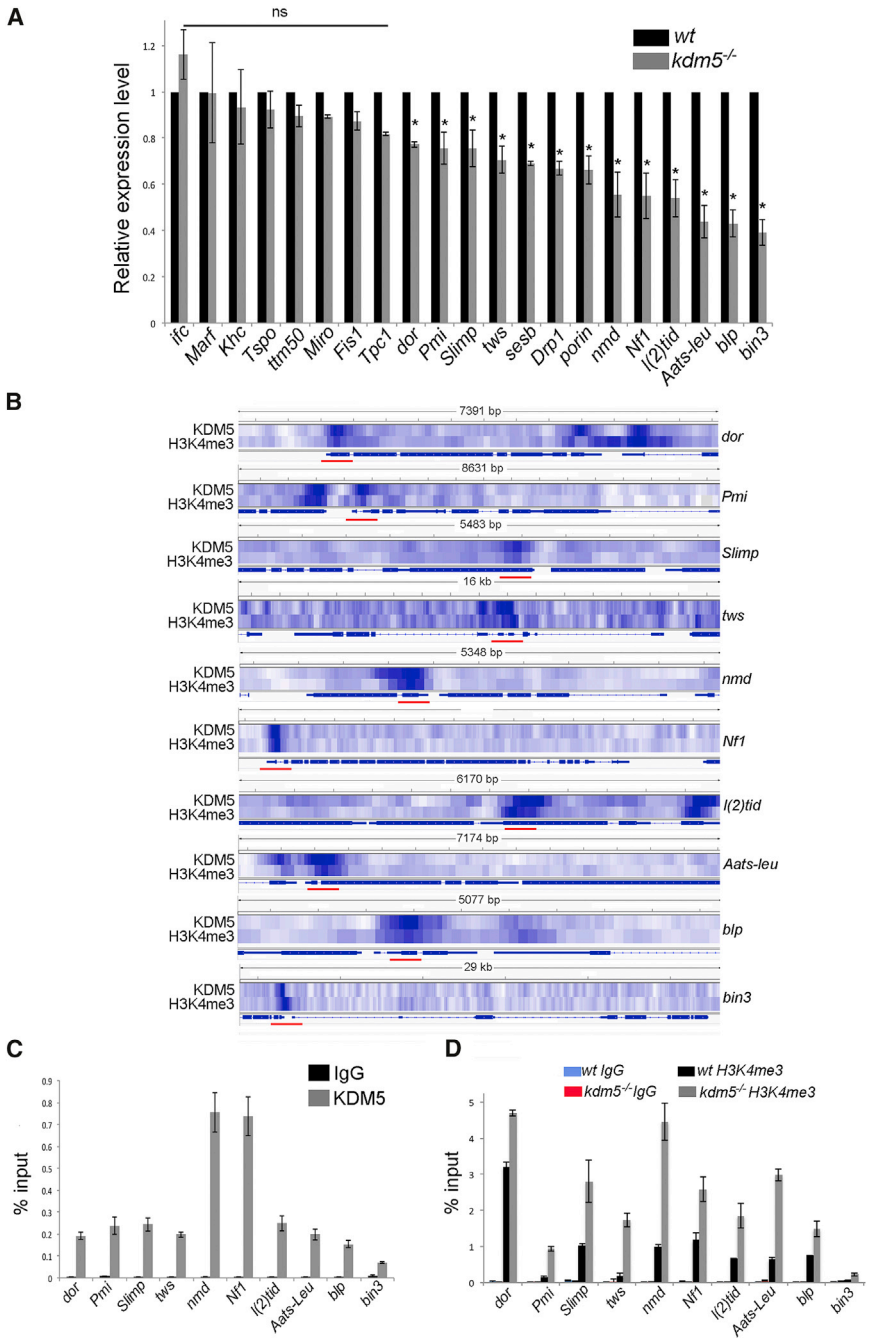

Figure 2. KDM5 Directly Regulates Genes Required for Mitochondrial Function

(A) Real-time PCR of genes indicated in *kdm5*$^{K6801/10424}$ adults shown relative to wild-type (*w*^{1118}). Genes were normalized to *rp49* and shown as relative expression in *kdm5* mutants (*p < 0.05).

(B) Heatmap showing overlapping KDM5 and H3K4me3 peaks at target genes. Red bars show regions used for ChIP-PCR validation shown in (C) and (D).

(C) ChIP-PCR using anti-HA (KDM5) and IgG control shows KDM5 enrichment at targets.

(D) ChIP-PCR using anti-H3K4me3 or control IgG from wild-type (*w*^{1118}) and *kdm5*$^{K6801/10424}$ mutant adults is shown.

Mitochondria from wild-type animals were round and evenly distributed between the myofibrils (Figures 3A and 3B). In contrast, *kdm5* mutant flies had irregularly shaped mitochondria that were larger than those of wild-type flies, while other cellular structures appeared normal (Figures 3C and 3D). Consistent with the mitochondrial defects of *kdm5* mutants interfering with the function of this organelle, total levels of ATP were decreased ~50% (Figure 3E). Interestingly, *kdm5* mutants did not show altered levels of lactic acid, suggesting that they do not (or are unable to) generate ATP through anaerobic glycolysis to compensate for reduced mitochondrial ATP output (Figure 3F). The ability to climb (negative geotaxis) is often affected in flies with mitochondrial or ATP production defects (Fergestad et al., 2008). Consistent with this correlation, *kdm5* mutant flies were significantly slower at climbing (Figure 3G).

One key metabolic pathway that occurs in the mitochondria is the tricarboxylic acid (TCA) cycle that serves as a hub to integrate carbohydrate, fat, and protein metabolism. To test whether the TCA cycle was affected in *kdm5* mutants, we quantitated levels of citrate and found it was 2.5-fold higher than in wild-type animals (Figure 3H). We also observed that several TCA cycle enzymes were upregulated in *kdm5* mutants, but these changes to gene expression were mostly indirect (Table S2). In addition to being a TCA cycle intermediate, citrate is a precursor for de novo synthesis of fatty acids that are necessary for membrane integrity and signaling. Examining the levels of 87 types of glycerophospholipids in *kdm5* mutants revealed that levels of long-chain glycerophospholipids were significantly increased (>38 carbons; Figure 3I). Shorter-chain glycerophospholipids (<38 carbons), lysophosphatidylcholine lipids, and sphingolipids were unaffected, suggesting that only a subset of lipids were altered in *kdm5* mutants (Figure 3I). Other metabolic pathways that feed into or out of the TCA cycle, such as levels of amino acids and biogenic amines, also were altered in *kdm5* mutants (Table S3).

An important function of the TCA cycle is to convert NAD+ to NADH, which then serves as an electron donor in ATP production generated through the electron transport chain. A breakdown in the TCA cycle would be expected to decrease the conversion of NAD+ to NADH and alter the redox state of the cell. Consistent with this expectation, *kdm5* mutants had a 3-fold increase in

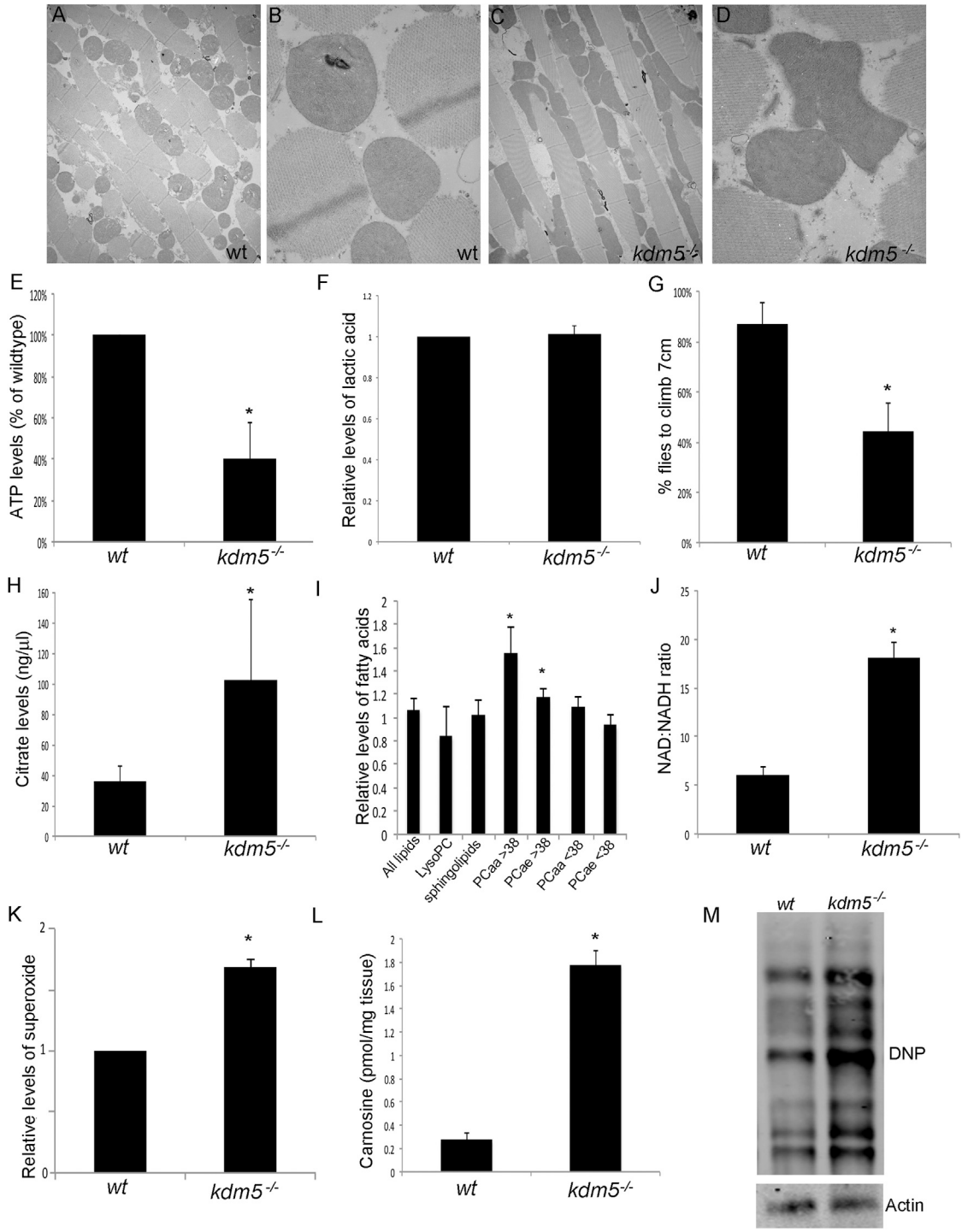

Figure 3. The *kdm5* Mutant Adults Have Mitochondrial and Metabolic Defects

(A and B) Transmission electron microscopy (TEM) images show 5,000 (A) and 10,000 (B) magnifications of mitochondria within thoracic muscles from wild-type (w^{1118}) flies.

(C and D) TEM images from $kdm5^{K6801/10424}$ mutant flies are shown.

(E) ATP levels in $kdm5^{K6801/10424}$ mutant flies are shown as percentage of wild-type and normalized to the total protein levels (*$p < 0.01$).

(F) Lactic acid levels in $kdm5^{K6801/10424}$ adults relative to w^{1118} are shown.

(G) Quantitation the number of wild-type (w^{1118}) or $kdm5^{K6801/10424}$ flies that climb 7 cm in 20 s after being tapped to the bottom of the vial is shown (*$p < 0.001$).

(H) Citrate levels (ng/µl) in wild-type and $kdm5^{K6801/10424}$ mutant flies are shown (*$p < 0.01$).

(legend continued on next page)

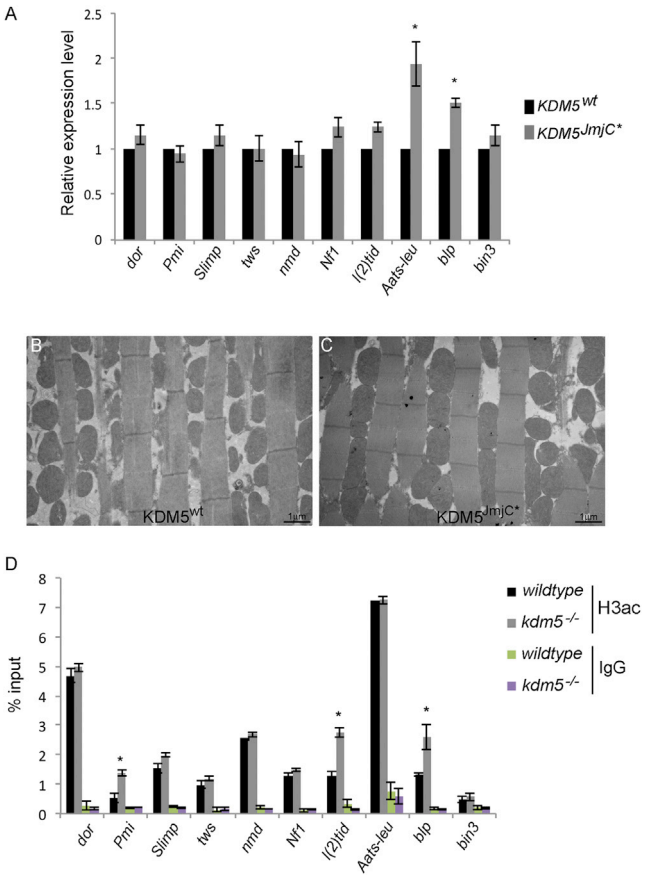

Figure 4. KDM5-Mediated Regulation of Mitochondrial Function Genes Is Independent of Its Demethylase Activity

(A) Real-time PCR analyses of the genes indicated in demethylase-inactive adults (described in Li et al., 2010; $kdm5^{JmjC*}$) relative to wild-type (w^{1118}). Each gene was normalized to *rp49* and is shown as relative expression in $kdm5^{JmjC}$ mutants (*p < 0.05).

(B and C) TEM images show 5,000 magnifications of mitochondria within thoracic muscles from $kdm5^{K6801}$ mutant flies rescued by a wild-type KDM5 transgene ($KDM5^{WT}$; B) and $kdm5^{JmjC}$ mutant flies (C).

(D) ChIP-PCR showing levels of histone H3 acetylation using a pan-acetyl antibody in wild-type and $kdm5^{K6801/10424}$ flies. IgG is a negative control. ChIP-PCR fragments are indicated in Figure 2B (*p < 0.05).

the ratio of NAD to NADH (Figure 3J). Through a number of different mechanisms, defective mitochondria also can lead to increased levels of potentially toxic reactive oxygen species (Cui et al., 2012). *kdm5* mutants had superoxide levels that were 1.6-fold higher than wild-type, suggesting that they experience increased oxidative stress in the absence of any exogenous stress source (Figure 3K). Consistent with this, the antioxidant stress indicator carnosine was increased 8-fold and global levels of oxidized proteins 2-fold (Figures 3L and 3M). *kdm5* mutants, therefore, have physical mitochondrial abnormalities and significant disruptions to metabolic processes related to energy production.

KDM5 Activation of Mitochondrial Function Genes Is Dependent on Its C-terminal PHD Motif and Independent of Its JmjC Domain Histone Demethylase Activity

To test the extent to which the demethylase activity was required for the gene expression changes observed, we examined flies specifically lacking KDM5-dependent enzymatic activity (Li et al., 2010). Of the ten genes related to mitochondrial function tested, eight were unaffected in demethylase-inactive flies while the remaining two genes were slightly upregulated (Figure 4A). The histone demethylase activity of KDM5 is, therefore, not required for the activation of these target genes. Consistent with this, we did not observe mitochondrial abnormalities in the thoracic muscles of demethylase-inactive flies (Figures 4B and 4C).

One of the means by which KDM5 can activate transcription is by increasing promoter histone H3 acetylation by inhibiting HDACs (DiTacchio et al., 2011; Lee et al., 2009). To test whether this mechanism plays a role in the activation of mitochondrial function genes, we tested whether levels of promoter H3 acetylation were decreased in *kdm5* mutant flies. Seven of the ten genes examined had no change in promoter histone H3 acetylation and the remaining three showed a slight increase (Figure 4D). KDM5-mediated activation of these genes, therefore, does not occur through changes to histone acetylation.

Because KDM5 binding correlated with H3K4me3, a chromatin mark bound by the C-terminal PHD3 motif of KDM5, we next tested the functional significance of this activity. To abolish H3K4me2/3 binding, we made two different mutations in PHD3 based on structural data from human KDM5A (Wang et al., 2009) and tested their ability to bind histone peptides in vitro (Figure 5A). Mutating tryptophan 1771 to alanine (W1771A) eliminated PHD3 binding to both di- and trimethylated H3K4 (Figure 5B). Altering glutamate and tryptophan at amino acid positions 1780 and 1781 to alanine (EW1780A) reduced binding to H3K4me2 and H3K4me3, but not as dramatically as W1771A. We therefore generated flies endogenously expressing full-length $KDM5^{W1771A}$ using a genomic rescue transgene approach that we used previously (Li et al., 2010). The only source of KDM5 in $kdm5^{W1771A}$ flies harbored the PHD3 mutation and was expressed at physiological levels using its endogenous promoter (Figure 5C). Flies harboring a wild-type version of the KDM5 genomic transgene served as a control for these analyses.

The $kdm5^{W1771A}$ homozygous flies eclosed at a slightly reduced Mendelian ratio, but surviving adults appeared

(I) Levels of distinct lipid subtypes in $kdm5^{K6801/10424}$ mutant flies relative to wild-type. LysoPC, lysophosphatidylcholine acyls (fatty acids generated as intermediate products); PCaa, phosphatidylcholine acyl molecules; PCae, phosphatidylcholine acyl-alkyl molecules. Numbers (<38 and >38) indicate number of carbon atoms in fatty acid chain (*p < 0.01).

(J) Ratio of NAD+ to NADH in wild-type (w^{1118}) and $kdm5^{K6801/10424}$ mutant flies is shown (*p < 0.001).

(K) Levels of superoxide as assayed by MitoSOX in $kdm5^{K6801/10424}$ mutant flies relative to wild-type are shown (*p < 0.05).

(L) Levels of the antioxidant carnosine (pmol/mg tissue) in wild-type and $kdm5^{K6801/10424}$ mutant flies are shown (*p < 0.001).

(M) Detection of oxidized proteins in wild-type and $kdm5^{K680/104241}$ mutant fly heads using oxyblot is shown (2-fold increase).

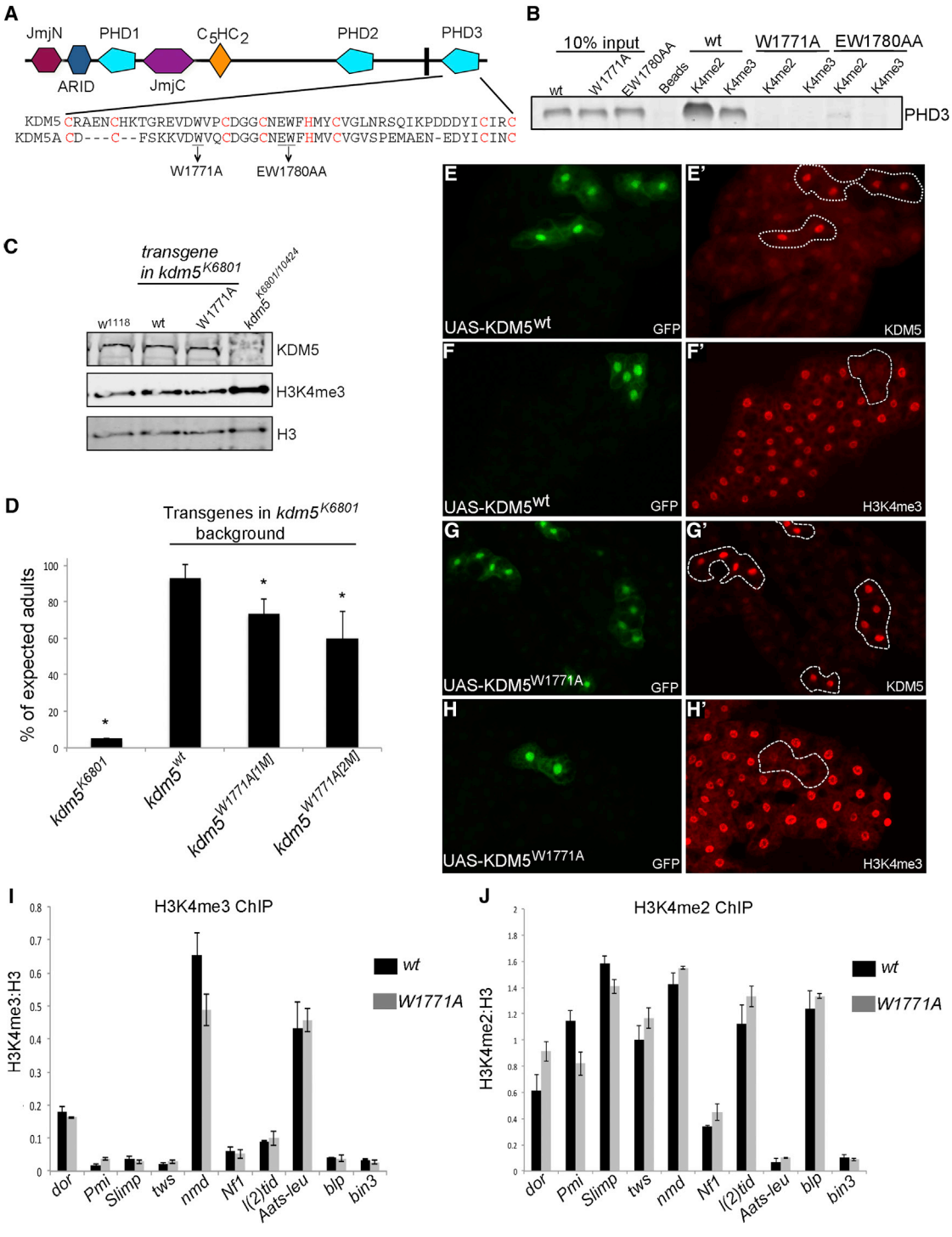

Figure 5. The *kdm5* Mutant Flies Unable to Bind H3K4me2/3 Retain Demethylase Activity

(A) Schematic of the PHD3 region of KDM5. Amino acids required for KDM5A binding to H3K4me2/3 are underlined and for zinc coordination in red (Wang et al., 2009).

(B) In vitro binding between biotinylated histone H3 peptides di- or trimethylated at lysine 4 (H3K4me2 and H3K4me3) and GST-PHD3. The interaction between KDM5 and H3K4me2 and H3K4me3 is abolished by GST-PHD3^{W1771A} and reduced by GST-PHD3^{EW1780AA}.

(C) Western from adult heads showing levels of KDM5, H3K4me3, and histone H3. H3 and H3K4me3 are two different channels from the same western blot. The H3K4me3:H3 ratio is increased in *kdm5*$^{K6801/10424}$ flies ($1.6^{\pm 0.3}$-fold).

(legend continued on next page)

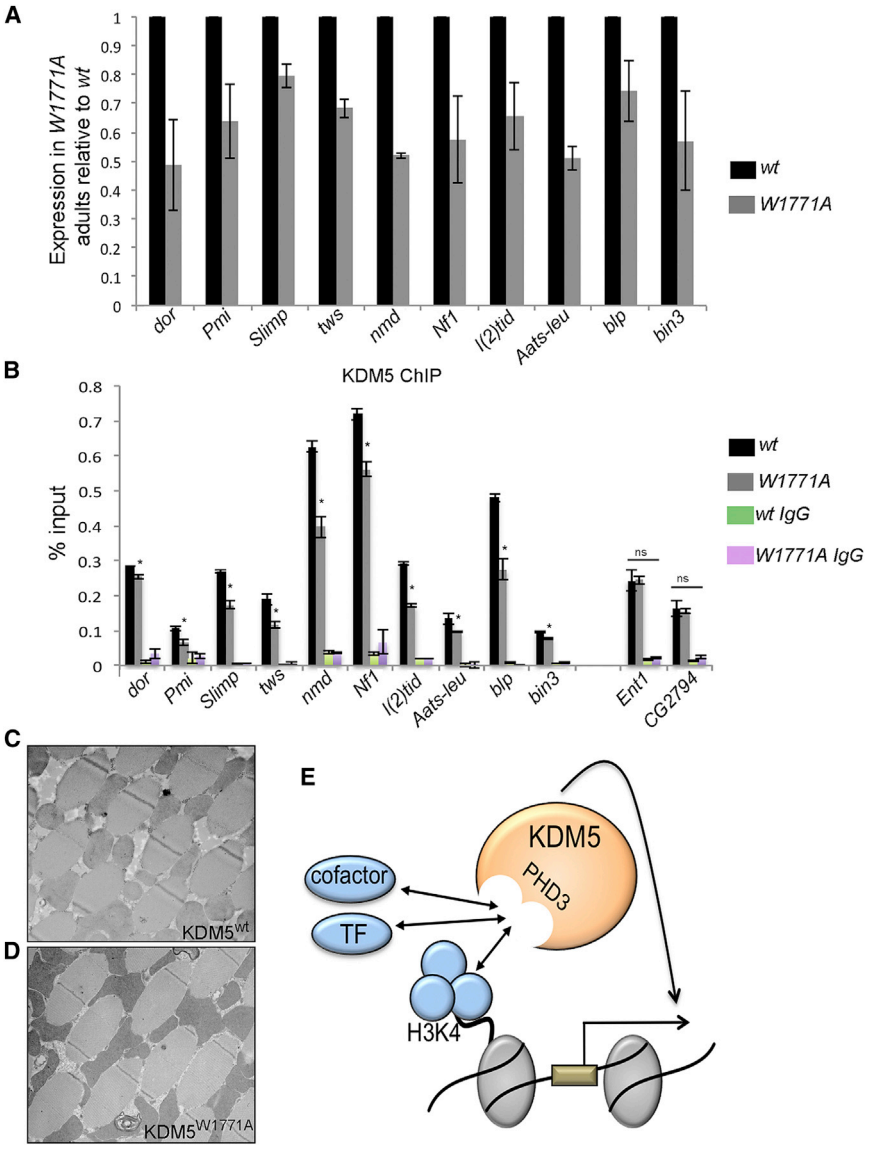

Figure 6. The PHD3 Motif of KDM5 Is Important for Gene Activation

(A) Real-time PCR comparing mRNA levels of direct KDM5 genes in flies lacking H3K4me2/3 binding (*kdm5*^{W1771A}; W1771A) and wild-type (*kdm5* mutant flies rescued by a wild-type transgene). All genes shown are significantly downregulated in *kdm5*^{W1771A} flies ($p < 0.05$).

(B) Anti-KDM5 ChIP-PCR analyses of binding at the target genes indicated in wild-type flies and *kdm5*^{W1771A} mutant flies are shown (*$p < 0.05$).

(C and D) TEM images show 5,000 magnifications of mitochondria within thoracic muscles from wild-type flies (KDM5^{WT}; C) and *kdm5*^{W1771A} mutant flies (KDM5^{W1771A}; D).

(E) Model for KDM5 function. KDM5 recruitment to its target mitochondrial function genes is regulated in part through recognition of the chromatin mark H3K4me3, but PHD3-mediated interaction(s) with as yet unidentified transcription factor(s) (TF) and transcriptional co-factors are also likely to be crucial.

morphologically normal (Figure 5D). Interestingly, in contrast to *kdm5* mutants that showed increased global levels of H3K4me3 due to the loss of demethylase activity, *kdm5*^{W1771A} animals did not have altered global levels of H3K4me3 (Figure 5C). Because PHD3 binds to the target substrate of KDM5's demethylase activity, we took two additional approaches to examine whether the PHD3 motif influenced the enzymatic activity of KDM5. First, we overexpressed KDM5^{W1771A} in fat body cells using the UAS/Gal4 system and found that was able to demethylate H3K4me3 in a manner similar to wild-type KDM5 (Figures 5E–5H). Second, we examined promoter proximal H3K4me3 by ChIP in *kdm5*^{W1771A} mutant flies and found that in, contrast to loss of KDM5 that results in increased H3K4me3, mutating the PHD3 motif had no effect on promoter H3K4me3 (Figure 5I). H3K4me2, which also is bound by PHD3, also is unaltered in *kdm5*^{W1771A} mutant flies (Figure 5J). The PHD3 motif of KDM5, therefore, acts independently of the JmjC domain-encoded demethylase activity.

To determine the extent to which H3K4me3 binding was required for transcriptional regulation by KDM5, we tested target gene expression levels in *kdm5*^{W1771A} flies. All ten mitochondrial-related genes examined were downregulated in *kdm5*^{W1771A} flies (Figure 6A). KDM5 promoter recruitment also was significantly attenuated at *dor*, *Pmi*, *Slimp*, *tws*, *nmd*, *Nf1*, *l(2)tid*, *Aats-leu*, *blp*, and *bin3* (Figure 6B). To test if H3K4me3 recognition contributed to KDM5 recruitment at a target gene not related to mitochondrial activity, we examined binding to the promoter of the gene *Equilibrative nucleoside transporter 1*

(D) Number of *kdm5*^{K6801} homozygous flies observed without a genomic rescue transgene (*kdm5*^{K6801}), with a wild-type rescue transgene (*kdm5*^{wt}) and two independent insertions of a kdm5^{W1771A} transgene (1M and 5M) is shown (*$p < 0.01$).

(E–H) Clones of fat body cells marked by the presence of GFP that express wild-type KDM5 or KDM5^{W1771A}. *hs*-FLP; UAS-KDM5 (or UAS-KDM5^{W1771A}) females were crossed to actin > CD2 > Gal4, UAS-GFP males. Transgene-expressing cells are shown by the co-expression of GFP (E, F, G, and H). Anti-KDM5 is shown in (E') and (G') and anti-H3K4me3 in (F') and (H').

(I) ChIP-PCR analyses of H3K4me3 levels at KDM5 target genes in wild-type flies (*kdm5*^{K6801} mutant flies rescued by a wild-type genomic rescue construct [*wt*]) and *kdm5*^{W1771A} mutant flies. No significant changes were observed.

(J) ChIP-PCR analyses of H3K4me2 levels in wild-type and *kdm5*^{W1771A} mutant flies are shown.

(*Ent1*). Interestingly, KDM5 binding to this gene was unaltered in *kdm5*^{W1771A} mutant flies (Figure 6B). We also tested KDM5 binding to the promoter of the putative kinase *CG2794*, which has lower H3K4me3 levels, and found it to be unaffected in *kdm5*^{W1771A} mutants (Figure 6B). Consistent with the gene expression changes observed, *kdm5*^{W1771A} mutant flies had deformed mitochondria in their thoracic muscles (Figures 6C and 6D). H3K4me3 recognition by KDM5, therefore, plays an important role in the regulation of gene expression, and abrogating this activity results in mitochondrial abnormalities.

To ascertain whether the effect on KDM5 recruitment was specific to PHD3 or a general feature of PHD motifs, we examined the function of the N-terminal PHD motif (PHD1) that binds to histone H3 that is unmethylated at lysine 4 (H3K4me0) (Li et al., 2010; Torres et al., 2015). Similar to our analyses of PHD3, we generated flies expressing a mutant form of KDM5 unable to bind H3K4me0 at endogenous levels (*kdm5*^{W490A}; Figures S5A–S5C). We also overexpressed KDM5^{W490A} using a UAS transgene and found that, in contrast to deleting the PHD1 motif (Li et al., 2010), specifically abrogating H3K4me0 binding did not affect the demethylase activity of KDM5 (Figures S5D–S5G). Importantly, ChIP analyses demonstrated that KDM5^{W490A} was recruited to mitochondrial function genes in a manner similar to wild-type KDM5 (Figure S5H). The PHD1 and PHD3 motifs, therefore, have distinct functions, and only PHD3 is involved in recruiting KDM5 to the promoters of mitochondrial function genes.

Because abrogating KDM5-dependent recognition of H3K4me2/3 attenuated, but did not abolish, promoter binding (Figure 6B), chromatin recognition is not the sole means by which KDM5 is recruited to its targets. The PHD3 motif of KDM5 is, therefore, likely to interact with additional factors critical for transcriptional activation. One possibility for this is that the PHD3 of KDM5 interacts with transcription factor(s) necessary for gene activation. We used MEME-ChIP to determine whether KDM5-regulated mitochondrial function genes were enriched for DNA motifs that could contribute to gene activation. Three DNA motifs were identified by these analyses, none of which have been associated with a known transcription factor (Figures S6A–S6D). All ten mitochondrial function genes contained motif 3 (TGGAAA), seven contained motif 2 (GGAACANGGA), and six contained motif 1 (GGGGCAGA); four promoters had all three motifs. Additionally, based on the observation that the H3K4me3-binding PHD motif of KMT2A also interacts with the transcriptional cofactor Cyp33 (Ali et al., 2014), the PHD3 of KDM5 may be required for the recruitment of cofactor(s) that are limiting for gene activation. These possibilities are summarized in Figure 6E.

DISCUSSION

Based on genome-wide transcriptome and ChIP data, we demonstrate a direct, critical role for KDM5 in the activation of genes required for the integrity and functioning of mitochondria. Focusing on ten mitochondrial function genes, we found that KDM5-dependent target gene activation was independent of its well-established histone demethylase activity. Taken with previous reports from us and others (Catchpole et al., 2011; Li et al., 2010; Secombe et al., 2007), these data further support the view that KDM5 has essential gene regulatory functions that lie outside of its JmjC domain-encoded enzymatic activity. Consistent with non-demethylase functions playing important roles, we observed a striking correlation between KDM5 binding and the presence of the active chromatin mark H3K4me3. Further support for a significant connection between KDM5 binding and the presence of H3K4me3 comes from studies of mammalian KDM5 proteins (Kidder et al., 2014; Lopez-Bigas et al., 2008; Ram et al., 2011) and of *Drosophila* KDM5 in larval wing imaginal disc cells (Lloret-Llinares et al., 2012). Although the target genes are distinct in different tissues and at different developmental stages, the binding of KDM5 proteins to H3K4me3-enriched regions of the genome appears to be highly conserved.

Importantly, we extend these correlative data by specifically addressing the functional importance of PHD3-mediated recognition of H3K4me2/3 by KDM5 in vivo. Flies harboring a mutation in the PHD3 of KDM5 that abrogated H3K4me2/3 binding showed decreased binding to, and expression of, mitochondrial function genes. Moreover, this was specific to PHD3, as a mutation in the PHD1 motif of KDM5 that binds H3K4me0 did not alter KDM5 recruitment. These data demonstrate that the C-terminal PHD motif (PHD3) is a vital contributor to promoter recruitment and to gene activation by KDM5. Importantly, because both the PHD1 and PHD3 domains behaved independently of the JmjC demethylase domain, our data reinforce the notion that KDM5 proteins regulate transcription by distinct mechanisms that utilize the activity of different domains.

The *kdm5* mutant flies had physically abnormal mitochondria in addition to metabolic defects that led to decreased ATP production, altered lipid metabolism, and increased levels of oxidative stress. These phenotypes were likely to be caused by the combined dysregulation of numerous KDM5 targets, as individual genes showed relatively mild (~2-fold) changes in transcript levels. Significantly, we expect that our observed regulation of mitochondrial function genes is a conserved function of KDM5 proteins, as KDM5A knockdown in SAOS-2 cells that lacked the KDM5-interacting protein pRB showed a long rod mitochondrial phenotype (Lopez-Bigas et al., 2008; Váraljai et al., 2015). However, in contrast to our findings in flies, KDM5A knockdown cells did not show any change in the levels of reactive oxygen species, possibly due to compensation from other KDM5 family proteins. In the case of KDM5A, the only characterized direct target was *Mitofusin 2* (*Mnf2*), whose expression was repressed by KDM5A (Lopez-Bigas et al., 2008). The *Drosophila* paralog of *Mnf2*, *Mitochondrial assembly regulatory factor* (*Marf*), was bound by KDM5 in our ChIP-seq data, but its expression was not altered in whole animals. KDM5 may, therefore, regulate *Marf* in a tissue-specific manner in flies.

Our observation that KDM5 affects mitochondrial function is particularly relevant to our understanding of the link between overexpression of KDM5A or KDM5B and the genesis and progression of a number of different types of cancers (Blair et al., 2011). KDM5A- and KDM5B-overexpressing tumors are often resistant to traditional chemotherapy treatments (Blair et al., 2011). This effect has been characterized in some detail in KDM5B-overexpressing melanomas, where drug resistance is

linked to the survival of a small population of slowly dividing cells (Roesch et al., 2010, 2013). Proteomic analyses of KDM5B-overexpressing cells revealed an increase in mitochondrial bioenergy that correlated with resistance to chemotherapy drugs (Roesch et al., 2013). However, no gene expression changes were reported to account for the link between KDM5B and changes to mitochondrial activity. Based on our data, we suggest that KDM5B may directly regulate genes required to increase mitochondrial activity and that this is key to the survival of this subset of slow-growing cells that can cause therapy resistance. We further propose that the effects of KDM5B on mitochondrial activity may be PHD3 dependent. In this regard it is interesting to note that the PHD3 motif previously has been linked to cancer, as this domain of KDM5A forms part of a leukemia-causing fusion protein (van Zutven et al., 2006; Wang et al., 2009). In addition, our previous studies showed that the PHD3 motif of KDM5 is required for the induction of cell growth in concert with the oncoprotein transcription factor Myc (Li et al., 2010). Together, these data show the importance of chromatin recognition by KDM5, and they suggest a direct role for dysregulation of PHD motif-mediated H3K4me3 recognition in cancer.

Mitochondrial dysfunction is also an emerging theme among conditions that affect neuronal functioning, including fragile X-related syndromes, Down syndrome, Alzheimer's disease, Rett syndrome, and some autism spectrum disorders (De Felice et al., 2012; Pagano and Castello, 2012; Yan et al., 2013). Mutations in KDM5A and KDM5B are found in patients with autosomal recessive intellectual disability, and mutations in KDM5C are found in those with the X-linked form of this disease (Vallianatos and Iwase, 2015). Reduced mitochondrial function and/or increased oxidative stress may contribute to the neuronal phenotypes observed in these patients. It is also noteworthy that our analyses of directly regulated KDM5 target genes revealed significant enrichment for several transcription factors critical for neuronal development and function. In particular, factors such as Lola (Longitudinals lacking) and Ttk (Tramtrack) are required for dendrite development (Iyer et al., 2013; Parrish et al., 2006). Because dendrite abnormalities are found in KDM5C knockdown cells (Iwase et al., 2007), the dysregulation of KDM5-Lola and KDM5-Ttk target genes may contribute to the cognitive pathologies seen in patients with mutation in KDM5 family genes.

EXPERIMENTAL PROCEDURES

Fly Strains

Fly strains were obtained from Bloomington stock center. Individually, $kdm5^{10424}$ and $kdm5^{K6801}$ homozygotes survive at less than 5%, but $kdm5^{10242}/kdm5^{K6801}$ is a hypomorphic allelic combination in which adults survive at ~50% expected frequency (30% of wild-type protein levels) (Li et al., 2010; Liu et al., 2014; Secombe et al., 2007). The wild-type untagged, HA-tagged *kdm5*, and demethylase-inactive ($kdm5^{JmjC*}$) genomic rescue transgenes were reported previously (Li et al., 2010; Liu et al., 2014). The PHD3 and PHD1 mutant genomic rescue transgenes ($gKDM5^{W1771A}$ and $gKDM5^{W490A}$) were generated by site-directed mutagenesis. The $gKDM5^{W1771A}$ transgene insertion numbers 1M, 2M, and 5M were tested and behaved indistinguishably. The $gKDM5^{W490A}$ 8M or 9M was used. UAS-KDM5 was generated using the pUASt vector. UAS-$KDM5^{W1771A}$ and UAS-$KDM5^{W490A}$ were generated by site-directed mutagenesis. Transgenic flies were generated by The Best Gene.

RNA-Seq and ChIP-Seq Analyses

RNA-seq analyses were carried out comparing wild-type (w^{1118}) flies and $kdm5^{K6801/10424}$ flies that were 1–3 days old. ChIP-seq using anti-KDM5 (using w^{1118} flies) and anti-HA (using genomic tagged KDM5:HA flies) were carried out using 1- to 3-day-old flies. Details of RNA-seq and ChIP-seq analyses are described in the Supplemental Experimental Procedures.

Real-Time PCR

Total RNA (1 μg) was reverse transcribed using Verso cDNA kit (Thermo Scientific) with oligo (dt) primer. The qRT-PCR reactions were performed in triplicate as described previously (Liu et al., 2014). Primer sequences are provided in Table S4.

ChIP

ChIP-PCR binding signals were calculated as a percentage of input DNA as described previously (Liu et al., 2014). IgG was used as a negative control. Primers used for ChIP-PCR are shown in Table S4.

Quantitation of ATP, Citrate, and Lactic Acid Levels and the Ratio of NAD to NADH

ATP concentration was determined using the ATP bioluminescence assay kit HS II (Invitrogen). Values were normalized to protein concentration. Citrate and lactic acid concentrations were determined using kits from Sigma (MAK057 and MAK064, respectively). The ratio of NAD/NADH was determined using the NAD/NADH assay kit II (Sigma MAK037).

Superoxide Quantitation

MitoSOX (Invitrogen) fluorescence was quantitated from control (w^{1118}) and $kdm5^{K6801/10424}$ mutant flies using isloated mitochondria as described previously (Tang et al., 2009).

Histone Binding

Histone-binding assays were carried out as described previously (Li et al., 2010).

Westerns and Immunofluorescence

The KDM5 antibody has been described previously (Secombe et al., 2007). Anti-H3K4me2, H3K4me3, and H3 were obtained from Active Motif. Western analysis was carried out using standard protocols, infrared-conjugated secondary antibodies (LI-COR Biosciences), and band intensity quantitated using LI-COR Odyssey version 3.0 software. Immunofluorescence of larval tissue was carried out as described in Secombe et al. (2007).

Metabolite Analyses

Wild-type (w^{1118}) or $kdm5^{K6801/10424}$ mutant adults were homogenized in 2.5 mM ammonium acetate in methanol and analyzed using ultraperformance liquid chromatography-tandem mass spectrometry (UPLC-MS/MS, Acquity UPLC Xevo TQ MS). Assay procedures and metabolite nomenclature have been described previously (Gieger et al., 2008; Illig et al., 2010). Six biological replicates of pooled quality control (QC) samples (for each genotype) were analyzed to calculate the %CV for each metabolite.

Electron Microscopy

Thoraxes from 1- to 3-day-old flies were fixed in 2% paraformaldehyde, 2.5% glutaraldehyde, 5 mM $CaCl_2$, and 0.1 mM sodium cacodylate for 24 hr at 4°C. This was followed by 2-hr post-fixation in 2.5% glutaraldehyde, 0.8% osmium tetroxide, and 0.1 mM sodium cacodylate at 4°C. Ultrathin sections were cut on a Reichert Ultracut UCT, stained with uranyl acetate followed by lead citrate, and viewed on a JEOL 1200EX transmission electron microscope at 80 kv.

Negative Geotaxis Assays

Flies were tapped down to the bottom of an empty standard plastic food vial and the number of flies that climbed 7 cm within 20 s quantified. Females (80: ten flies per vial, eight biological replicates) were scored for each genotype.

Statistical Analyses

Unless otherwise indicated, data are presented as mean ± SEM from at least three independent biological replicates (each done in triplicate). Statistical significances were evaluated using Student's t test and one-way ANOVA analyses using GraphPad Prism software. Statistical analyses of Mendelian ratios were carried out using chi-square test.

ACCESSION NUMBERS

The accession number for the RNA-seq and ChIP-seq reported in this paper is GEO: GSE70591.

SUPPLEMENTAL INFORMATION

Supplemental Information includes Supplemental Experimental Procedures, six figures, and four tables and can be found with this article online at http://dx.doi.org/10.1016/j.celrep.2015.11.007.

AUTHOR CONTRIBUTIONS

X.L. and J.S. conceived, designed, and performed the experiments and analyzed the data. J.S. and X.L. wrote the paper.

ACKNOWLEDGMENTS

The authors thank J.S. lab members and Hardik Shah and Yongping Qui from the Einstein Diabetes Research and Training Center (DRTC) Metabolomics Core Facility. This work was supported by NIH grant R01GM112783 to J.S.

Received: July 31, 2015
Revised: October 5, 2015
Accepted: October 31, 2015
Published: December 3, 2015

REFERENCES

Albert, M., Schmitz, S.U., Kooistra, S.M., Malatesta, M., Morales Torres, C., Rekling, J.C., Johansen, J.V., Abarrategui, I., and Helin, K. (2013). The histone demethylase Jarid1b ensures faithful mouse development by protecting developmental genes from aberrant H3K4me3. PLoS Genet. *9*, e1003461.

Ali, M., Hom, R.A., Blakeslee, W., Ikenouye, L., and Kutateladze, T.G. (2014). Diverse functions of PHD fingers of the MLL/KMT2 subfamily. Biochim. Biophys. Acta *1843*, 366–371.

Barrett, A., Santangelo, S., Tan, K., Catchpole, S., Roberts, K., Spencer-Dene, B., Hall, D., Scibetta, A., Burchell, J., Verdin, E., et al. (2007). Breast cancer associated transcriptional repressor PLU-1/JARID1B interacts directly with histone deacetylases. Int. J. Cancer *121*, 265–275.

Benevolenskaya, E.V. (2007). Histone H3K4 demethylases are essential in development and differentiation. Biochem. Cell Biol. *85*, 435–443.

Blair, L.P., Cao, J., Zou, M.R., Sayegh, J., and Yan, Q. (2011). Epigenetic Regulation by Lysine Demethylase 5 (KDM5) Enzymes in Cancer. Cancers (Basel) *3*, 1383–1404.

Cao, J., Liu, Z., Cheung, W.K., Zhao, M., Chen, S.Y., Chan, S.W., Booth, C.J., Nguyen, D.X., and Yan, Q. (2014). Histone demethylase RBP2 is critical for breast cancer progression and metastasis. Cell Rep. *6*, 868–877.

Catchpole, S., Spencer-Dene, B., Hall, D., Santangelo, S., Rosewell, I., Guenatri, M., Beatson, R., Scibetta, A.G., Burchell, J.M., and Taylor-Papadimitriou, J. (2011). PLU-1/JARID1B/KDM5B is required for embryonic survival and contributes to cell proliferation in the mammary gland and in ER+ breast cancer cells. Int. J. Oncol. *38*, 1267–1277.

Cui, H., Kong, Y., and Zhang, H. (2012). Oxidative stress, mitochondrial dysfunction, and aging. J. Signal Transduct. *2012*, 646354.

De Felice, C., Signorini, C., Leoncini, S., Pecorelli, A., Durand, T., Valacchi, G., Ciccoli, L., and Hayek, J. (2012). The role of oxidative stress in Rett syndrome: an overview. Ann. N Y Acad. Sci. *1259*, 121–135.

DiTacchio, L., Le, H.D., Vollmers, C., Hatori, M., Witcher, M., Secombe, J., and Panda, S. (2011). Histone lysine demethylase JARID1a activates CLOCK-BMAL1 and influences the circadian clock. Science *333*, 1881–1885.

Eissenberg, J.C., Lee, M.G., Schneider, J., Ilvarsonn, A., Shiekhattar, R., and Shilatifard, A. (2007). The trithorax-group gene in Drosophila little imaginal discs encodes a trimethylated histone H3 Lys4 demethylase. Nat. Struct. Mol. Biol. *14*, 344–346.

Fergestad, T., Olson, L., Patel, K.P., Miller, R., Palladino, M.J., and Ganetzky, B. (2008). Neuropathology in Drosophila mutants with increased seizure susceptibility. Genetics *178*, 947–956.

Gieger, C., Geistlinger, L., Altmaier, E., Hrabé de Angelis, M., Kronenberg, F., Meitinger, T., Mewes, H.W., Wichmann, H.E., Weinberger, K.M., Adamski, J., et al. (2008). Genetics meets metabolomics: a genome-wide association study of metabolite profiles in human serum. PLoS Genet. *4*, e1000282.

Gildea, J.J., Lopez, R., and Shearn, A. (2000). A screen for new trithorax group genes identified little imaginal discs, the Drosophila melanogaster homologue of human retinoblastoma binding protein 2. Genetics *156*, 645–663.

Illig, T., Gieger, C., Zhai, G., Römisch-Margl, W., Wang-Sattler, R., Prehn, C., Altmaier, E., Kastenmüller, G., Kato, B.S., Mewes, H.W., et al. (2010). A genome-wide perspective of genetic variation in human metabolism. Nat. Genet. *42*, 137–141.

Iwase, S., Lan, F., Bayliss, P., de la Torre-Ubieta, L., Huarte, M., Qi, H.H., Whetstine, J.R., Bonni, A., Roberts, T.M., and Shi, Y. (2007). The X-linked mental retardation gene SMCX/JARID1C defines a family of histone H3 lysine 4 demethylases. Cell *128*, 1077–1088.

Iyer, E.P., Iyer, S.C., Sullivan, L., Wang, D., Meduri, R., Graybeal, L.L., and Cox, D.N. (2013). Functional genomic analyses of two morphologically distinct classes of Drosophila sensory neurons: post-mitotic roles of transcription factors in dendritic patterning. PLoS ONE *8*, e72434.

Kidder, B.L., Hu, G., and Zhao, K. (2014). KDM5B focuses H3K4 methylation near promoters and enhancers during embryonic stem cell self-renewal and differentiation. Genome Biol. *15*, R32.

Klein, B.J., Piao, L., Xi, Y., Rincon-Arano, H., Rothbart, S.B., Peng, D., Wen, H., Larson, C., Zhang, X., Zheng, X., et al. (2014). The histone-H3K4-specific demethylase KDM5B binds to its substrate and product through distinct PHD fingers. Cell Rep. *6*, 325–335.

Lee, N., Zhang, J., Klose, R.J., Erdjument-Bromage, H., Tempst, P., Jones, R.S., and Zhang, Y. (2007). The trithorax-group protein Lid is a histone H3 trimethyl-Lys4 demethylase. Nat. Struct. Mol. Biol. *14*, 341–343.

Lee, N., Erdjument-Bromage, H., Tempst, P., Jones, R.S., and Zhang, Y. (2009). The H3K4 demethylase lid associates with and inhibits histone deacetylase Rpd3. Mol. Cell. Biol. *29*, 1401–1410.

Li, L., Greer, C., Eisenman, R.N., and Secombe, J. (2010). Essential functions of the histone demethylase lid. PLoS Genet. *6*, e1001221.

Liu, X., Greer, C., and Secombe, J. (2014). KDM5 interacts with Foxo to modulate cellular levels of oxidative stress. PLoS Genet. *10*, e1004676.

Lloret-Llinares, M., Pérez-Lluch, S., Rossell, D., Morán, T., Ponsa-Cobas, J., Auer, H., Corominas, M., and Azorín, F. (2012). dKDM5/LID regulates H3K4me3 dynamics at the transcription-start site (TSS) of actively transcribed developmental genes. Nucleic Acids Res. *40*, 9493–9505.

Lopez-Bigas, N., Kisiel, T.A., Dewaal, D.C., Holmes, K.B., Volkert, T.L., Gupta, S., Love, J., Murray, H.L., Young, R.A., and Benevolenskaya, E.V. (2008). Genome-wide analysis of the H3K4 histone demethylase RBP2 reveals a transcriptional program controlling differentiation. Mol. Cell *31*, 520–530.

Machanick, P., and Bailey, T.L. (2011). MEME-ChIP: motif analysis of large DNA datasets. Bioinformatics *27*, 1696–1697.

Nègre, N., Brown, C.D., Ma, L., Bristow, C.A., Miller, S.W., Wagner, U., Kheradpour, P., Eaton, M.L., Loriaux, P., Sealfon, R., et al. (2011). A cis-regulatory map of the Drosophila genome. Nature *471*, 527–531.

Nishibuchi, G., Shibata, Y., Hayakawa, T., Hayakawa, N., Ohtani, Y., Sinmyozu, K., Tagami, H., and Nakayama, J. (2014). Physical and functional interactions between the histone H3K4 demethylase KDM5A and the nucleosome

remodeling and deacetylase (NuRD) complex. J. Biol. Chem. *289*, 28956–28970.

Outchkourov, N.S., Muiño, J.M., Kaufmann, K., van Ijcken, W.F., Groot Koerkamp, M.J., van Leenen, D., de Graaf, P., Holstege, F.C., Grosveld, F.G., and Timmers, H.T. (2013). Balancing of histone H3K4 methylation states by the Kdm5c/SMCX histone demethylase modulates promoter and enhancer function. Cell Rep. *3*, 1071–1079.

Pagano, G., and Castello, G. (2012). Oxidative stress and mitochondrial dysfunction in Down syndrome. Adv. Exp. Med. Biol. *724*, 291–299.

Parrish, J.Z., Kim, M.D., Jan, L.Y., and Jan, Y.N. (2006). Genome-wide analyses identify transcription factors required for proper morphogenesis of Drosophila sensory neuron dendrites. Genes Dev. *20*, 820–835.

Ram, O., Goren, A., Amit, I., Shoresh, N., Yosef, N., Ernst, J., Kellis, M., Gymrek, M., Issner, R., Coyne, M., et al. (2011). Combinatorial patterning of chromatin regulators uncovered by genome-wide location analysis in human cells. Cell *147*, 1628–1639.

Roesch, A., Fukunaga-Kalabis, M., Schmidt, E.C., Zabierowski, S.E., Brafford, P.A., Vultur, A., Basu, D., Gimotty, P., Vogt, T., and Herlyn, M. (2010). A temporarily distinct subpopulation of slow-cycling melanoma cells is required for continuous tumor growth. Cell *141*, 583–594.

Roesch, A., Vultur, A., Bogeski, I., Wang, H., Zimmermann, K.M., Speicher, D., Körbel, C., Laschke, M.W., Gimotty, P.A., Philipp, S.E., et al. (2013). Overcoming intrinsic multidrug resistance in melanoma by blocking the mitochondrial respiratory chain of slow-cycling JARID1B(high) cells. Cancer Cell *23*, 811–825.

Santos-Rosa, H., Schneider, R., Bannister, A.J., Sherriff, J., Bernstein, B.E., Emre, N.C.T., Schreiber, S.L., Mellor, J., and Kouzarides, T. (2002). Active genes are tri-methylated at K4 of histone H3. Nature *419*, 407–411.

Secombe, J., and Eisenman, R.N. (2007). The function and regulation of the JARID1 family of histone H3 lysine 4 demethylases: the Myc connection. Cell Cycle *6*, 1324–1328.

Secombe, J., Li, L., Carlos, L., and Eisenman, R.N. (2007). The Trithorax group protein Lid is a trimethyl histone H3K4 demethylase required for dMyc-induced cell growth. Genes Dev. *21*, 537–551.

Sharma, S.V., Lee, D.Y., Li, B., Quinlan, M.P., Takahashi, F., Maheswaran, S., McDermott, U., Azizian, N., Zou, L., Fischbach, M.A., et al. (2010). A chromatin-mediated reversible drug-tolerant state in cancer cell subpopulations. Cell *141*, 69–80.

Sims, R.J., 3rd, and Reinberg, D. (2006). Histone H3 Lys 4 methylation: caught in a bind? Genes Dev. *20*, 2779–2786.

Song, I.S., Jeong, J.Y., Jeong, S.H., Kim, H.K., Ko, K.S., Rhee, B.D., Kim, N., and Han, J. (2015). Mitochondria as therapeutic targets for cancer stem cells. World J. Stem Cells *7*, 418–427.

Tang, S., Le, P.K., Tse, S., Wallace, D.C., and Huang, T. (2009). Heterozygous mutation of Opa1 in Drosophila shortens lifespan mediated through increased reactive oxygen species production. PLoS ONE *4*, e4492.

Torres, I.O., Kuchenbecker, K.M., Nnadi, C.I., Fletterick, R.J., Kelly, M.J., and Fujimori, D.G. (2015). Histone demethylase KDM5A is regulated by its reader domain through a positive-feedback mechanism. Nat. Commun. *6*, 6204.

Vallianatos, C.N., and Iwase, S. (2015). Disrupted intricacy of histone H3K4 methylation in neurodevelopmental disorders. Epigenomics *7*, 503–519.

van Zutven, L.J., Onen, E., Velthuizen, S.C., van Drunen, E., von Bergh, A.R., van den Heuvel-Eibrink, M.M., Veronese, A., Mecucci, C., Negrini, M., de Greef, G.E., and Beverloo, H.B. (2006). Identification of NUP98 abnormalities in acute leukemia: JARID1A (12p13) as a new partner gene. Genes Chromosomes Cancer *45*, 437–446.

Váraljai, R., Islam, A.B., Beshiri, M.L., Rehman, J., Lopez-Bigas, N., and Benevolenskaya, E.V. (2015). Increased mitochondrial function downstream from KDM5A histone demethylase rescues differentiation in pRB-deficient cells. Genes Dev. *29*, 1817–1834.

Wang, G.G., Song, J., Wang, Z., Dormann, H.L., Casadio, F., Li, H., Luo, J.L., Patel, D.J., and Allis, C.D. (2009). Haematopoietic malignancies caused by dysregulation of a chromatin-binding PHD finger. Nature *459*, 847–851.

Yan, M.H., Wang, X., and Zhu, X. (2013). Mitochondrial defects and oxidative stress in Alzheimer disease and Parkinson disease. Free Radic. Biol. Med. *62*, 90–101.

Zou, S., Meadows, S., Sharp, L., Jan, L.Y., and Jan, Y.N. (2000). Genome-wide study of aging and oxidative stress response in Drosophila melanogaster. Proc. Natl. Acad. Sci. USA *97*, 13726–13731.